International Journal of Thermophysics, Vol. 23, No. 4, July 2002 (© 2002)

The Role of Adsorption and Phase Change Phenomena in the Thermophysical Characterization of Moist Porous Materials[1]

F. Scarpa[2, 3] and G. Milano[2]

Phase change phenomena in moist porous media with low liquid content, the typical condition of a porous body at ambient conditions and far from the contact of liquid water, are controlled by the shape of the adsorption isotherms and by the effective liquid-vapor thermodynamic condition within the pores. Usually, heat and mass transfer models are developed under the assumption of thermal and hygrometric equilibrium. This gives rise to an expression of the evaporation source that is too complex in view of the dynamic identification of thermophysical and transport properties of a porous material. In this study, the hypothesis of hygrometric equilibrium is dropped. The phase change rate is considered proportional to the amount of local nonequilibrium through an appropriate delay coefficient. This approach leads to a simple representation of the process and makes manageable the formulation of a coupled heat and mass transfer inverse problem. A comparison with a first group of experiments performed with an open-pore light insulating material (expanded perlite board) confirms the suitability of the proposed approach. However, the analysis shows that, for this material, phase change occurs not far from the hygrometric equilibrium.

KEY WORDS: evaporation source; heat and moisture transport; light insulators; porous media; thermophysical properties.

1. INTRODUCTION

Several studies and research efforts have been devoted to heat and mass transfer in porous media involving phase change phenomena and capillary

[1] Paper presented at the Fourteenth Symposium on Thermophysical Properties, June 25–30, 2000, Boulder, Colorado, U.S.A.

[2] DITEC - Università di Genova, Via All'Opera Pia 15 A, I-16145 Genova, Italy.

[3] To whom correspondence should be addressed. E-mail: fscarpa@ditec.unige.it

0195-928X/02/0700-1033/0 © 2002 Plenum Publishing Corporation

effects. The basic transport equations were described by Luikov [1] with a physical representation essentially based on the well-known governing point equations enhanced by empirical arguments. Whitaker [2] organized the subject into a rigorous theory; by an in-depth analysis and the systematic application of an averaging technique, a system of equations is derived which accurately describes the moisture transfer process. However, the application of such a complete description is very difficult and many simplifications and assumptions are usually made to practically implement the heat and mass transfer equations. A widely used approach, in case of slow drying processes at constant pressure, has been proposed by De Vries [3] and developed by Crausse et al. [4]. This simplified model gives satisfactory results in many practical situations but still presents great complexity in the expression of the mass diffusion coefficients due to the particular set of variables chosen to describe the process, i.e., temperature and total moisture. In case of small liquid content in a discontinuous state, a description in terms of temperature and vapor concentration leads to a more realistic and relatively simple representation of the process although the source of evaporation still retains a complex form.

In this work the authors propose the relaxation of the hypothesis of hygrometric equilibrium between liquid water and its vapor in the interior of the material. This approach has various purposes. The first, apart from any physical consideration, is to simplify the description of the source term, making more manageable the design of an inverse algorithm devoted to the reconstruction of the adsorption characteristics of a material from transient experiments. Moreover, the proposed transport model gives an opportunity to investigate the influence of a possible nonequilibrium effect on the temperature and moisture distributions inside a material subjected to transient drying experiments. To emphasize the role of the sorption isotherm and of the vapor diffusion, drying processes in the presence of small liquid contents are considered, so that the liquid phase is assumed immobile in the so-called pendular state.

2. HEAT AND MASS TRANSFER MODEL

The porous material is assumed to be homogeneous and isotropic. Heat and mass transfer is considered one dimensional and described in terms of temperature, liquid content, and vapor concentration. The liquid phase is considered immobile in a discontinuous state [5], and the total pressure of the gas phase is assumed uniform and constant. Gravity is neglected, and the convective terms in the energy equation are dropped. Although a unique value of temperature is used to describe both liquid and gas phases, the vapor density is not assumed equal to the equilibrium

density as it happens in the construction of the adsorption isotherms. Finally, hysteresis phenomena are ignored. We emphasize that, since the total gas pressure is assumed constant and the liquid in a pendular state, all the mass fluxes both in gas and liquid phase are absent. So parameters like permeability and suction characteristics are not involved in this analysis. According to the above assumptions, the one-dimensional differential heat and moisture transfer equations are expressed as follows:

$$\rho_0 \bar{c} \frac{\partial T}{\partial t} = \frac{\partial}{\partial z}\left(\lambda_{\text{eff}} \frac{\partial T}{\partial z}\right) - h_{\text{lv}} \dot{m}, \tag{1}$$

$$\rho_0 \frac{\partial u_2}{\partial t} = -\dot{m}, \tag{2}$$

$$\rho_0 u_\gamma \frac{\partial C}{\partial t} = \frac{\partial}{\partial z}\left(\rho_0 u_\gamma D_{\text{eff}} \frac{\partial C}{\partial z}\right) + (1 - C)\, \dot{m}, \tag{3}$$

where the subscripts have the meaning:

0: dry body	σ: solid phase
1: vapor	β: liquid phase (= 2)
2: liquid	γ: gas phase
4: dry air	

In Eqs. (1)–(3) T stands for temperature; u_2 is the liquid content defined as the mass ratio between liquid water and dry body, whose apparent density is ρ_0; C is the vapor concentration; $\bar{c}$ and λ_{eff} are the average specific heat and the effective thermal conductivity of the medium, respectively; and h_{lv} is the enthalpy of vaporization.

In Eq. (3) the effective diffusion coefficient D_{eff} is

$$D_{\text{eff}} = \frac{D_{1\text{–}4}}{\delta} \tag{4}$$

where δ is the tortuosity of the material while $D_{1\text{–}4}$, the Fick diffusion coefficient of water vapor in dry air, has been assumed as [6]

$$D_{1\text{–}4} = 2.17 \cdot 10^{-5} \left(\frac{T}{273.15}\right)^{2.7}$$

The term $\dot{m}$ corresponds to the evaporation source. It is assumed proportional to the difference between the equilibrium density of vapor and its actual density, i.e., to the amount of local nonequilibrium, through an appropriate time delay coefficient τ:

$$\dot{m} = \frac{1}{\tau}(\rho_s \varphi - \rho_l), \tag{5}$$

A similar expression for $\dot{m}$ is given in Ref. 7.

In Eq. (5) ρ_l is the vapor density and ρ_s is the saturation density for the case of a flat interface. The term φ represents the ratio between the equilibrium density in the interior of the body and ρ_s. It can be described as a function of liquid content and temperature through the adsorption isotherms of the investigated material:

$$\varphi = \varphi(u_2, T) \tag{6}$$

More precisely, the coefficient τ should be considered as a function of the evaporating surface per unit volume which is a function of u_2. Furthermore, preliminary studies on the subject show that the linear relation between $\dot{m}$ and $(\rho_s \varphi - \rho_l)$ seems to be valid only in the case of small departure from the hygrometric equilibrium. Equation (5) has been selected essentially for the sake of simplicity. In fact, the correct expression of the source term following the classic hypothesis of hygrometric equilibrium, that is $\rho_l = \rho_s \varphi$, is a complex function:

$$\dot{m} = F\left(\nabla \cdot \vec{j}_l, \nabla \cdot \vec{q}, \frac{\partial u_l}{\partial u}, \frac{\partial u_l}{\partial T}\right) \tag{7}$$

where $\vec{j}_l$ and $\vec{q}$ are the vapor and the heat flux, respectively.

Since the total moisture u is the sum of both the vapor and liquid contents:

$$u = u_1 + u_2 = \frac{\rho_1 \varepsilon_\gamma}{\rho_0} + \frac{\rho_2 \varepsilon_\beta}{\rho_0} \tag{8a}$$

the vapor content u_1 can be expressed as a function of u and T as:

$$u_1 = \frac{\rho_s(T)\, \varphi(u, T)}{\rho_0}\left(\frac{\alpha \rho_2 - u \rho_0}{\rho_2 - \rho_s(T)\, \varphi(u, T)}\right) \tag{8b}$$

Since an inverse algorithm requires the construction of the sensitivity equations by differentiating the process model with respect to all the unknown parameters β_j, we have to calculate the derivatives,

$$\frac{\partial \dot{m}}{\partial \beta_j} \tag{9}$$

The evaluation of such terms is very involved since most of the parameters β_j are used to describe the unknown shape of the adsorption characteristics of the material, that is, of the function φ. The simple form of Eq. (5) makes the construction of the sensitivity equations easier. This work should be considered a preliminary investigation about the best way to face the implementation of a complete inverse algorithm which is left for future work.

As known, the constant pressure hypothesis forces the removal of the gas-phase conservation equation. If the transport process is described in terms of the total moisture content u, the consequence of the above hypothesis is a non-conservation of the dry air alone. On the contrary, if the vapor concentration C is adopted, the constant pressure hypothesis gives rise to a non-conservation of humid rather than dry air. This fact better adheres to the real three-dimensional phenomenon where the total pressure tends to remain constant resulting from a molar escape of gas from the boundaries, that is, an escape of water vapor and dry air proportional to their concentration.

In Eq. (1) the average specific heat $\bar{c}$ is assumed as the following weighted mean:

$$\bar{c} = c_\sigma + u_1 c_1 + u_2 c_2 + u_4 c_4, \tag{10}$$

while the effective thermal conductivity is described as [8]:

$$\lambda_{\text{eff}} = \lambda_\sigma^* + \varepsilon_\beta \lambda_2 + \varepsilon_\gamma \frac{u_1 \lambda_1 + u_4 \lambda_4}{u_1 + u_4} \tag{11}$$

with $\lambda_\sigma^* = \varepsilon_\sigma \lambda_\sigma$.

The volumetric fractions ε_σ, ε_β, and ε_γ refer to solid, liquid, and gas phases, respectively.

Based on the knowledge of temperature, liquid content, and vapor concentration, we are able to calculate the following required quantities:

$$\varepsilon_\gamma = \alpha - \frac{\rho_0}{\rho_2} u_2; \qquad \rho_\gamma = \frac{p}{R_4 T} [1 - C(1 - R_1/R_4)]^{-1}; \qquad u_\gamma = \frac{\rho_\gamma \varepsilon_\gamma}{\rho_0};$$

$$u_1 = C u_\gamma; \qquad \rho_1 = C \rho_\gamma; \qquad u_4 = u_\gamma - u_1;$$

where α is the porosity of the material, p is the total pressure of the gas phase, and R_1 and R_4 are the particular constants for water vapor and dry air, respectively.

3. PHASE CHANGE EFFECTS

The proposed model has been preliminarily compared to the classic formulation given by De Vries and Crausse [3, 4] by means of simulated experiments at a quasi-equilibrium condition. The results, not reported here in detail, showed that if the value of the delay constant τ approaches zero, the temperature versus time histories given by the two models differ by less than 0.02 K over a wide range of the initial moisture content ($0.1 < \varphi_0 < 0.9$) and of the drying process rate (40 to 160 $K \cdot h^{-1}$). We note that, because of the explicit formulation adopted in the numerical solution, the constant τ cannot be reduced below a certain critical value depending on the time and space discretization interval, thermophysical properties, etc.

The typical effect of the moisture on the temperature response inside the material when the specimen is subjected to transient heating is shown in Fig. 1. Starting from an initial uniform temperature distribution, an

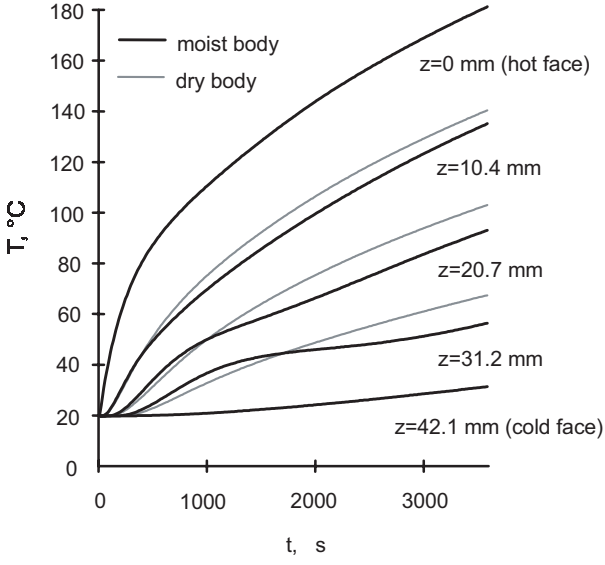

Fig. 1. Experimental temperature response of the material (EPB) at the boundaries and at the three inner locations in dry (dashed line, $\varphi_0 = 0.01$) and moist (continuous line, $\varphi_0 = 0.68$) conditions.

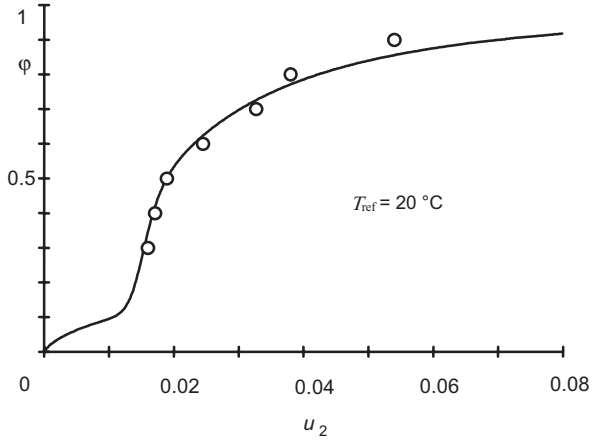

Fig. 2. Adsorption isotherm ($T = 20°C$) of the investigated material. Experimental points (○) and optimized curve.

exponential temperature increase on one surface ($z = 0$ mm) is imposed while the opposite surface ($z = 42.1$ mm) is maintained at the initial cold temperature. The temperature versus time histories on the boundary surfaces and at different elevations inside the material are reported. Dashed lines refer to the dry body, while continuous lines refers to the moist ($\varphi_0 = 0.68$) one.

The moist body was simulated by using the sorption characteristic depicted in Fig. 2, and the temperature dependence of $\varphi(u_2, T)$ has been obtained by means of the well known Kelvin relation so that:

$$\varphi(u_2, T) = \varphi(u_2, T_{\text{ref}})^{\frac{\sigma(T)}{\rho_\beta(T)\,T}\frac{\rho_\beta(T_{\text{ref}})\,T_{\text{ref}}}{\sigma(T_{\text{ref}})}}$$

where σ is the interfacial tension of water.

The dry thermophysical properties refer to a porous insulator described in detail in the next section.

The average difference between the two families of curves reported in Fig. 1 is about 7 K. With reference to the middle sensor, we note that in the first stage of the experiment, the temperature is greater than in the case of a dry body because of the condensation of vapor coming from the zone of the specimen nearest to the hot surface. Then, the temperature increase slows down from the effect of the evaporation, which, at that location, becomes intense after one third of the experiment duration. In the sequel the phase change reduces and an inflection point in the temperature-time

curve appears. We note that the difference between dry and moist temperature distributions is mainly due to the source term in the energy equation while the variation of the thermophysical properties due to the liquid content profile plays a secondary role.

Figure 3A shows the temperature and liquid distributions inside the specimen after 1800 s from the start of the experiment while in Fig. 3B the evaporation source is depicted to emphasize the close connection between phase change, liquid content, and temperature. One can see that the convexity of the temperature curve is opposite to the z-axis in the zone characterized by condensation. Two different evaporation fronts can be noted in both the liquid distribution and the evaporation source. The main front is typical for a fast drying process while the secondary one is due to the shape of the adopted adsorption isotherm. As a comparison, the temperature distribution for the case of a dry body is shown (dashed line) in Fig. 3A.

4. EXPERIMENTAL COMPARISON

To compare the proposed model to real drying experiments, we have to estimate, first of all, the dry thermophysical properties of the selected material: an open-cell light insulator, namely, EPB (expanded perlite board). Experience showed that heat transfer by radiation and convection is negligible for EPB so that, in a dry condition, a purely conductive model is appropriate.

The only unknown quantities in Eqs. (10) and (11) are c_σ and λ_σ^* which have been identified, as a function of temperature, by means of an inverse technique [9] applied on transient experiment in dry conditions. In this case, in fact, we have

$$c_{\text{dry}} = c_\sigma + c_4 \frac{\alpha}{\rho_0} \frac{p_4}{R_4 T} \qquad \lambda_{\text{dry}} = \lambda_\sigma^* + \alpha \lambda_4, \tag{12}$$

where p_4 is equal to the atmospheric pressure. During the same estimation procedure, the effective position of the sensors in the interior of the specimen has also been identified [10].

The transient experiments have been accomplished by means of the facility described in detail in Ref. 11. The specimen, placed inside an airtight thermostatted cylindrical vessel, is made of four disk shaped slices, each with a diameter $d \approx 240$ mm and a thickness $s \approx 10.5$ mm (total thickness, $L = 42.1$ mm). The specimen is sandwiched between two temperature controlled impermeable surfaces. The total time duration of the

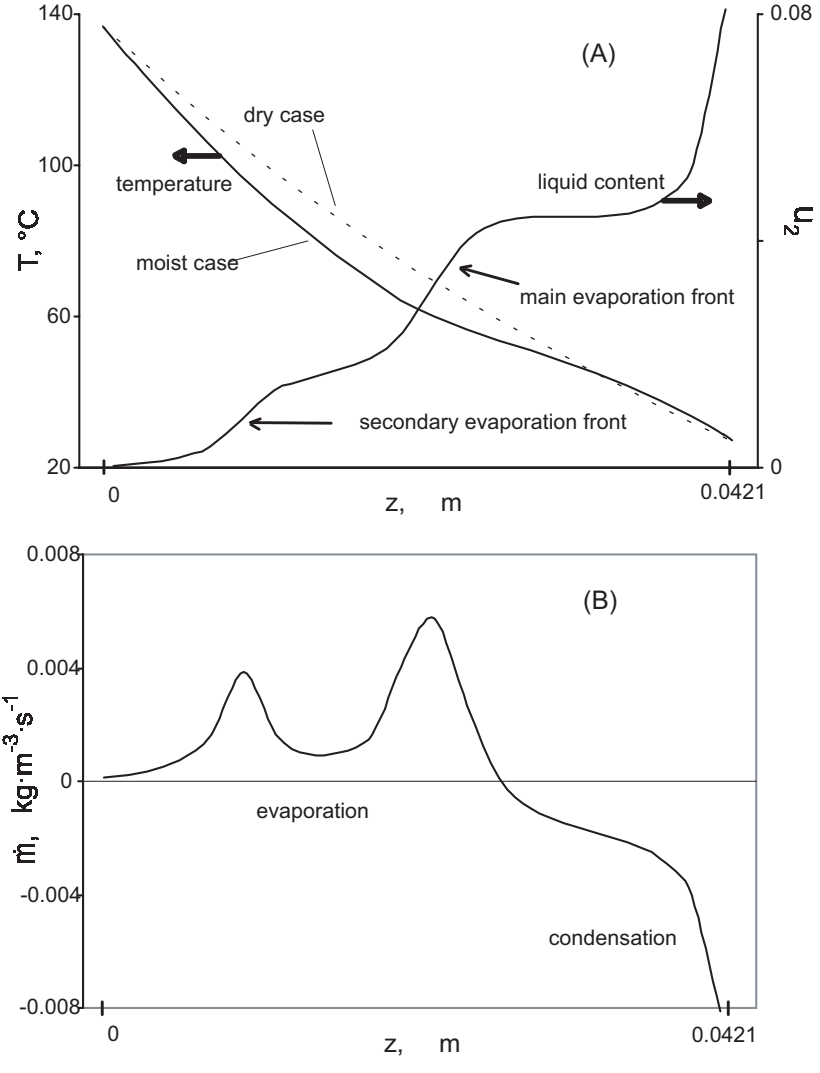

Fig. 3. Temperature and liquid water distributions (A) and evaporation source (B) at the middle of a simulated transient experiment (1800 s). Initial relative humidity $\varphi_0 = 0.75$. The dashed line in (A) refers to the dry case.

heating is $t_{exp} = 3600$ s, and temperature readings at the boundaries and in the interior of the specimen, at three different locations, are made every 2.5 s. Before the tests at a dry condition, the sample is kept at a temperature of 150°C and at a pressure of about 5 μbar for one week. Then the vessel is filled with dried air at 18°C, 1 bar and a relative humidity less than

0.4%. The specific heat and thermal conductivity of the dry material have been parameterized as follows:

$$c_{\text{dry}} = c_0 + c_1(T - T_{\text{ref}}) \tag{13}$$

$$\lambda_{\text{dry}} = \lambda_0 + \lambda_1(T - T_{\text{ref}}), \tag{14}$$

with

$$T_{\text{ref}} = 20°\text{C}$$

The reconstruction process gave us the following values for the parameters:

$$c_0 = 884 \text{ J} \cdot \text{kg}^{-1} \cdot \text{K}^{-1} \qquad c_1 = 3.320 \text{ J} \cdot \text{kg}^{-1} \cdot \text{K}^{-2}$$

$$\lambda_0 = 0.05 \text{ W} \cdot \text{m}^{-1} \cdot \text{K}^{-1} \qquad \lambda_1 = 1.09 \cdot 10^{-4} \text{ W} \cdot \text{m}^{-1} \cdot \text{K}^{-2}$$

and for the effective positions of the three inner sensors:

$$z_1 = 10.4 \text{ mm} \qquad z_2 = 20.7 \text{ mm} \qquad z_3 = 31.2 \text{ mm}$$

The apparent density $\rho_0 = 149 \text{ kg} \cdot \text{m}^{-3}$ of the dry material is obtained by weighing the specimen under vacuum while the porosity $\alpha = 0.94$ is derived from a knowledge of the material composition.

Moist transient experiments have been accomplished with the same experimental setup as used in the dry case. The initial, practically uniform, temperature distribution in the material covered the range 18 to 22°C, and the initial relative humidity of ambient air in equilibrium with the specimen has been varied from $\varphi_0 = 0.04$ up to $\varphi_0 = 0.75$. The transient drying is achieved by heating one face of the specimen so that an exponential temperature increment results up to a maximum temperature of the order of 70, 130, and 180°C. The opposite face is kept at nearly constant temperature.

To implement the model (Eqs. (1)–(3)), the tortuosity has been initially set to $\delta = 3$ [12] while the assumed adsorption characteristic ($T_{\text{ref}} = 20°\text{C}$) of the material is shown in Fig. 2, along with the experimental points evaluated by the climatic chamber method. In the lack of static data due to intrinsic limitations of the available climatic chamber, the particular shape of the curve for small liquid content has been chosen in such a way to minimize the differences between experimental and simulated temperatures in a transient regime.

A first group of 30 transient experiments has been performed with EPB. The tortuosity and the time delay constant have been varied to obtain a good fit between simulations and experiments.

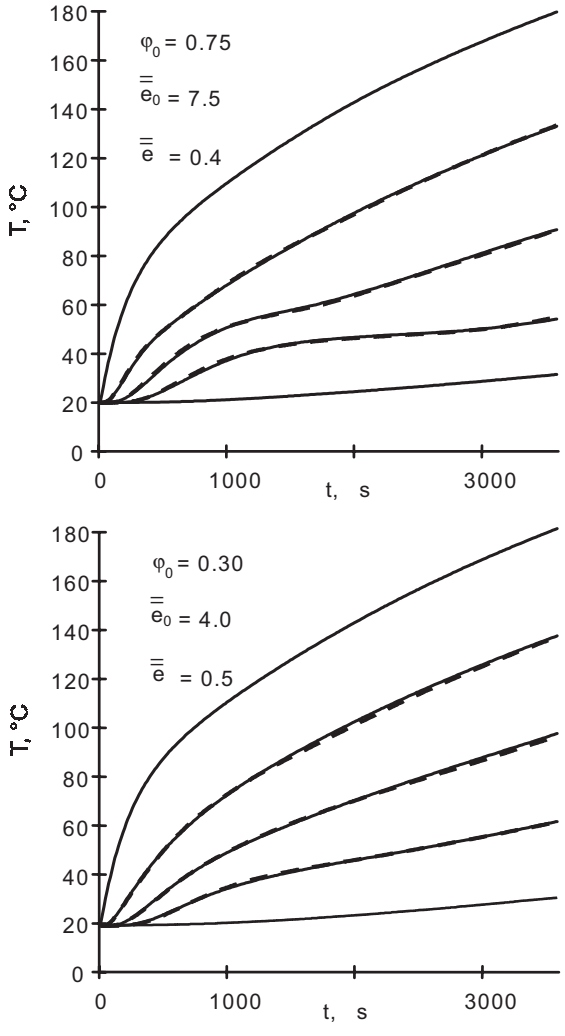

Fig. 4. Experimental (continuous line) and simulated (dashed line) temperature profiles. (A) $T_{max} = 180°C$, $\varphi_0 = 0.75$. (B) $T_{max} = 180°C$, $\varphi_0 = 0.3$. The profiles appear practically coincident.

The best results have been obtained with a tortuosity value $\delta \approx 3.5$ and $\tau \approx 0.3$ s. In all cases, the square root $\bar{\bar{e}}$ of the mean quadratic difference between simulated and real temperature distributions defined by Eq. (15) resulted in a value smaller than 0.6°C.

$$\bar{\bar{e}} = \sqrt{\frac{1}{N_t} \sum_{k=1}^{N_t} (T_{sim} - T_{exp})^2}, \tag{15}$$

where N_t is the total number of measurements.

Figure 4 shows the temperature profiles relative to a sharp transient in case of high (A) and low (B) initial moisture content. The initial relative humidity is 75 and 30%, respectively, and the liquid content for case (B) is practically one half of that for case (A). The figure reports the value $\bar{\bar{e}}$ and $\bar{\bar{e}}_0$, this last being a measure of the difference between dry and moist temperature profiles. In order to verify the attainment of initial thermo-hygrometric equilibrium between the specimen and the surrounding humid air, a series of test was performed by varying the preliminary stabilization period from ten days up to two months. The results reported in Table I refers to the same experimental conditions of Fig. 4A. As one can see, the average difference between simulation and experiment is practically the same in all the tests, showing that a period of about ten days is sufficient to reach thermo-hygrometric equilibrium inside the material.

As previously noted, the best agreement between experiments and numerical predictions has been obtained with a time delay $\tau \approx 0.3$ s. This small value suggests that, during the transient heating, phase change occurs for a condition near the hygrometric equilibrium. In fact, to observe effects of some relevance on the temperature distribution, the time delay constant should be greater than a few seconds. To give an idea of the influence of the time delay coefficient on the temperature history and on the phase change phenomena, a series of simulations was performed using all of the same thermophysical properties as before but increasing τ up to 30 s. The results reported in Fig. 5 refer to the middle of the specimen ($z = 20.7$ mm). Figure 5A shows the temperature-time variation while Fig. 5B depicts the

Table I. Repeatability Tests

Esperiment no.	Stabilization period (days)	Average temp. difference $\bar{\bar{e}}$ (K)
1	10	0.40
2	30	0.41
3	60	0.41

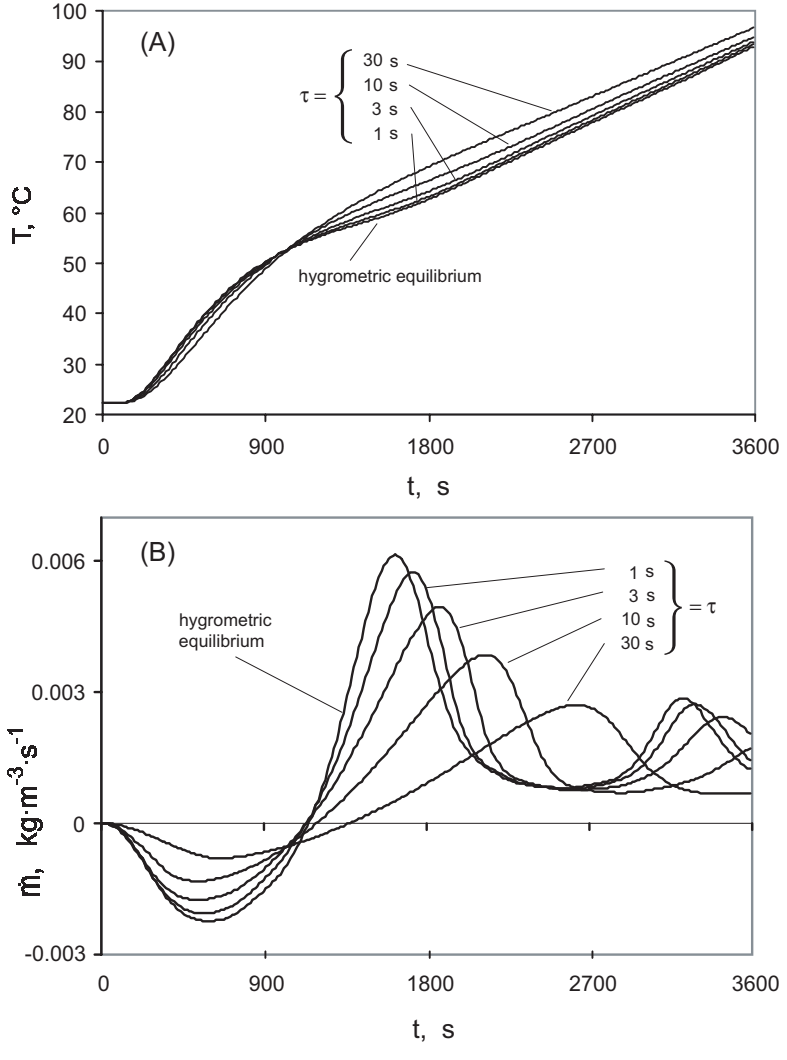

Fig. 5. Temperature (A) and evaporation source (B) as a function of time for increasing values of the time delay coefficient τ (simulated experiment, $z = 20.7$ mm, $\varphi_0 = 0.75$).

amount of evaporation. As the delay constant increases, the phase change phenomena are dumped. The effect on the evaporation front is pronounced: a time delay constant of a few seconds, for example three, in the source Eq. (5) causes a delay of about four minutes on the main evaporation front. The consequences on the temperature distribution are a decrease

of all the effects ascribable to the evaporation and depicted in Fig. 1 so that the inflection point vanishes.

5. CONCLUSION

A model for heat and mass transfer with phase change at a nonequilibrium condition inside a capillary porous material has been proposed. The model appears appropriate to describe heat and mass transfer with phase change in porous media. The relaxation of the hypothesis of local hygrometric equilibrium permits a great simplification in the expression of the evaporation source. The proposed approach leads to the construction of an inverse algorithm dedicated to the dynamic estimation of the shape of the sorption isotherm and of the other thermophysical and transport properties of a moist porous body. A first group of drying experiments performed with an open pore insulator (expanded perlite board) showed a time delay constant smaller than half a second. Therefore, for this material, phase change phenomena during transient heating occur not very far from the equilibrium condition. An interesting development of this study could consist of searching for some other material in which the nonequilibrium effect is more relevant. In any case the next important step is the construction of a complete inverse algorithm which allows us to better discriminate among the effects of the parameters controlling transport and phase change phenomena.

REFERENCES

1. A. V. Luikov, *Heat and Mass Tranfer in Capillary Porous Body* (Pergamon Press, Oxford, 1966).
2. S. Whitaker, *Advances in Heat Transfer* **13**:109 (1977).
3. D. De Vries, *Int. J. Heat Mass Transfer* **30**:1343 (1986).
4. P. Crausse, G. Bacon, and S. Bories, *Int. J. Heat Mass Transfer* **24**:991 (1980).
5. K. Vafai and Sarkar S., *J. Heat Transfer - Trans. ASME* **108**: 667 (1986).
6. S. Hokoi and M. K. Kumaran, *J. Thermal Insul. and Bldg. Envs.* **16**:263 (1993).
7. C. V. Le, N. G. Ly, and R. Postle, *Int. J. Heat Mass Transfer* **38**:81 (1995).
8. N. E. Wijeysundera, *J. Thermal Insul. and Bldg. Envs.* **19**:348 (1996).
9. G. Milano, F. Scarpa, and G. Timmermans, in *Thermal Conductivity, Vol. 22,* T. W. Tong, ed. (Technomic Publishing Co., Lancaster, Pennsylvania, 1994), pp. 263–274.
10. F. Scarpa, R. Bartolini, and G. Milano, *High Temp.-High Press.* **23**:633 (1991).
11. G. Milano, R. Bartolini, and F. Scarpa, *High Temp.-High Press.* **26**:177 (1994).
12. F. A. L. Dullien, in *Porous Media, Fluid Transport and Pore Structure* (Academic Press, New York, 1979), p. 225.